Kinetic Mapping of the Antibody Combining Site by Chemical Relaxation Spectrometry[†]

David Haselkorn, Suzan Friedman, David Givol, and Israel Pecht[*]

ABSTRACT: The antibody–hapten interaction was studied using protein-315, a mouse myeloma immunoglobulin possessing specificity toward the 2,4-dinitrophenyl (Dnp) moiety, and 38 different nitrophenyl ligands that consisted of three different groups into which systematic variations were introduced. (a) Nitrophenyl ligands differing in the number and position of the nitro groups or in the nature of the substituent on the aromatic ring. (b) Ligands with substitutions on the 1-amino group of 2,4-dinitroaniline. These comprised monosubstitutions by alkyl chains (branched and unbranched) that included carboxylate and ammonium groups, and disubstitutions with methyl and ethyl groups. (c) α-*N*-Dnp derivatives of glycine and glycylglycine, of D- and L-alanine, and its diastereoisomeric dipeptides (DD-, LL-, DL-, and LD-alanylalanine). The specific rates of binding and dissociation between protein-315 and these series of ligands were determined by the temperature-jump, chemical relaxation technique and then compared with their equilibrium binding constants as determined by fluorescence quenching. Large variations were observed in both specific rates of binding (k_{12}^*) and dissociation (k_{21}^*) when ligands of different structure were compared. This demonstrates that any explanation of the interaction between the ligand and the binding site in terms of the equilibrium constant only, is insufficient. The correlation between the structural features of these ligands and their specific rate constants enabled the kinetic mapping of the binding site of the protein. A model was then built in which the antibody combining site was divided into four "subsites of interaction," whose properties, size, and relative location with respect to the Dnp binding subsite were evaluated. The four subsites defined were: the 2,4-dinitrophenyl subsite (S_1), the first hydrophobic subsite (S_2), the second hydrophobic subsite (S_3), and the positive subsite (S_4). The minimal dimensions of the site so measured were 12 × 6 Å.

The interaction between antibody and hapten exhibits high affinity and specificity which springs from three-dimensional complementarity. Some parameters of the specificity have been analyzed by static methods (*e.g.*, equilibrium dialysis, fluorescence quenching, inhibition of precipitation) for a large series of antibodies and systematically modified haptens (Pressman and Grossberg, 1968). However, a deeper insight into the nature of these interactions can be achieved by resolving the elementary steps of the binding process.

Early attempts to study the kinetics of the reaction between the hapten 4-(4′-aminophenylazo)phenylarsonic acid and its homologous antibody with the aid of cathode ray polarography were made by Schneider and Sehon (1961). Lower limiting values of 10^6 M^{-1} sec^{-1} and 1 sec^{-1} were calculated for the rate constants k_{12}^* and k_{21}^*, respectively.[1] The antibody–hapten reaction was formulated as a reversible single step equilibrium. Sturtevant *et al.* (1961) and Day *et al.* (1962, 1963) studied the association of 2-(2,4-dinitrophenylazo)-1-naphthol-3,6-disulfonic acid and N^ϵ-Dnp[2]-lysine and N^ϵ-Dnp-aminocaproic acid with antibodies specific to N^ϵ of the Dnp moiety, by using the stopped-flow technique. Their results supported Schneider and Sehon's mechanism and they were able to compute a limiting binding rate constant close to 1 × 10^8 M^{-1} sec^{-1}. This method was applied recently by Barisas *et al.* (1974) to study the initial rates of binding 2,4-dinitrophenyl and 2,4,6-trinitrophenyl derivatives to their antibodies. Values of the same order of magnitude for the specific binding rate constants were found.

$$\mathrm{Ab} + \mathrm{H} \underset{k_{21}^*}{\overset{k_{12}^*}{\rightleftharpoons}} \mathrm{AbH} \qquad (1)$$
$$K = k_{12}^*/k_{21}^*$$

The temperature-jump method developed by Eigen and Maeyer (1963) has so far been applied to the study of two classes of antibodies. Those antibody–hapten systems in which conventionally induced, heterogeneous antibodies were used, and those consisting of an homogeneous IgA (protein-315) and its Dnp ligands (Pecht *et al.*, 1972a,b; Hochman *et al.*, 1972). The three induced heterogeneous antibody–hapten systems studied were: (i) anti-phenyl arsonate (Froese *et al.*, 1962), (ii) anti-*p*-nitrophenyl (Froese and Sehon, 1965; Froese, 1968), and (iii) anti-2,4-dinitrophenyl (Froese, 1968; Kelly *et al.*, 1971).

The information gained from these studies can be summarized as follows. (a) Only a single chemical relaxation effect was observed over a broad concentration range. (b) From the dependence of the relaxation times on free protein and hapten concentrations a single-step binding mechanism (eq 1) was deduced. (c) The second-order rate constants for the association step were in the range of 10^7–10^8 M^{-1} sec^{-1}, whereas the dissociation rate constants measured varied over three orders of magnitude and were the main cause for the changes in the overall equilibrium constant. These findings argue strongly against any major conformational change occurring during the reaction.

Kelly *et al.* (1971) found a twofold increase in k_{12}^* for the reaction between the Fab′ fragment of an induced anti-Dnp

---

[†] From the Department of Chemical Immunology, The Weizmann Institute of Science, Rehovot, Israel. *Received November 5, 1973.* This work has been supported by a grant from the Volkswagenwerk foundation and Grant No. AI 11453-01 from the National Institutes of Health. The grants are gratefully acknowledged.

[1] The notation of the experimentally observed rate constants is k_{12}^* and k_{21}^* for the binding and the dissociation, respectively. K_{st} is the association constant determined by fluorescence quenching.

[2] Abbreviations used are: Dnp, 2,4-dinitrophenyl; N_2phF, 1-fluoro-2,4-dinitrobenzene; alanine (LL), L-alanyl-L-alanine; alanine (DD), D-alanyl-D-alanine; alanine (LD), L-alanyl-D-alanine; alanine (DL), D-alanyl-L-alanine; BADL, N^α-bromoacetyl-N^ϵ-Dnp-L-lysine.

antibody and its hapten, when compared with the k_{12}^* measured for the reaction between the same hapten and the intact antibody molecule. No such difference was observed by Pecht *et al.* (1972a) for an homogeneous, monomeric, intact protein-315, its Fab′ fragment, or its polymeric form with the respective ligand, except for a slight increase in the specific rate of binding of a Dnp derivative to its Fv fragment (mol wt 25,000) (Inbar *et al.*, 1972; Hochman *et al.*, 1972). In both examples (Kelly *et al.*, 1971; Hochman *et al.*, 1972) the increase in k_{12}^* was attributed to a greater accessibility of the binding site and not to any type of conformational change. A conformational change was proposed (Barisas *et al.*, 1973) to occur in the reaction between anti-Dnp antibodies and the cross-reacting hapten, 2,4,6-trinitrophenylaminocaproic acid, since k_{12}^* for the Tnp ligand was smaller than k_{12}^* for the Dnp ligand. In these authors' opinion, this difference reflects a delay due to a time requiring structural change in the anti-Dnp binding site.

The dimensions and properties of the binding or catalytic site of antibodies and enzymes were probed by correlating the static equilibrium binding constants (K) of a series of systematically varied ligands with their structure and chemical properties (Kabat, 1960; Schechter and Berger, 1967, 1968; Abramovitz *et al.*, 1967; Pressman and Grossberg, 1968; Cuatrecasas *et al.*, 1968; Sharon and Chipman, 1969; Berger and Schechter, 1970; Schechter, 1970, 1972; Atlas *et al.*, 1970). In these studies, based on the contribution of the different groups in the ligand to the binding constant, the subsite concept was introduced as a tool to describe and analyze the nature of the binding site. However, the equilibrium constant K is defined for a reversible single-step reaction by k_{12}/k_{21}, and variations in K may result from changes in k_{12}, in k_{21}, or in both. Hence, correlating the variation in the structural parameters of the ligand with the changes in the overall equilibrium constant (K) provides only limited information. By the chemical relaxation method, both specific rates which determine the equilibrium constant can be evaluated directly. Thus, the correlation between the structural features of series of systematically modified ligands and their specific rates of interaction with the homogeneous protein is more meaningful in trying to resolve different interactions, and to map them in the combining site (Pecht and Haselkorn, 1971; Haselkorn *et al.*, 1971; Pecht *et al.*, 1972b).

The binding site mapped in this study was of protein-315; an IgA immunoglobulin produced by mouse plasma cell tumor, MOPC-315, that has a uniform primary structure (Potter *et al.*, 1964; Kunkel, 1965). It has been shown to bind polynitrophenyl ligands with high affinity to its homogeneous binding sites (Eisen *et al.*, 1970; Underdown *et al.*, 1971; Pecht *et al.*, 1972a). The mapping was accomplished by measuring the rates of interaction between protein-315 and 38 different ligands varying in size, charge, and spatial orientations.

Experimental Section

Materials. Protein-315 in its reduced alkylated monomeric form was prepared from the serum of tumor-bearing mice as previously described (Haimovich *et al.*, 1970; Inbar *et al.*, 1971).

Reagents. 2,4-Dinitroaniline, 2,4,6-trinitrotoluene, *p*-nitroaniline, 2,4-dinitrobenzene, 2,4-dinitrophenol, cyclohexylamine, *tert*-butylamine, isopropylamine, benzylamine, and 2,4-dinitrophenetole were purchased from Eastman Organic Chemicals; β-alanine, glycylglycine, 2,4-dinitrotoluene, 2,4-dinitrophenylhydrazine, and ethylamine were purchased from BDH Biochemicals; N_2PhF, 2,6-dinitroaniline, methylamine, *sec*-butylamine, *n*-propylamine, *n*-hexylamine, 1,2-ethylenediamine, and 1,3-propylenediamine were purchased from Fluka, AG; 2,6-dinitroaniline was purchased from Organic Research Chemicals; the Dnp derivatives of β-alanine, ε-aminocaproic, γ-aminobutyric, and δ-aminovaleric were purchased from Sigma Chemicals Co., and were found to be pure by thin-layer chromatography (tlc) (CCl_4–CH_3OH–CH_3COOH, 95:4:1).

Synthesis of Ligands. 1-N-2,4-Dinitrophenyl Derivatives of Methylamine, Ethylamine, Propylamine, Butylamine, Isopropylamine, sec-Butylamine, Isobutylamine, tert-Butylamine, Dimethylamine, and Diethylamine. A solution of 20 mmol of the respective alkylamine dissolved in 10 ml of 0.05 M $NaHCO_3$ was treated with 10 mmol of N_2phF dissolved in 10 ml of dioxane. The reaction mixture was stirred overnight at room temperature, and then evaporated *in vacuo*. The oily residue was dissolved in hot ethanol and was allowed to cool and crystallize at room temperature and then left at 4°. The solution was filtered; the yellow crystalline Dnp derivative was collected, recrystallized from hot ethanol, washed with water, and dried *in vacuo*. All the products were checked for purity by tlc (plates were developed in CCl_4–CH_3OH–CH_3COOH (95:4:1 or chloroform) and elementary analysis (Table I).

1-N-2,4-Dinitrophenylhexylamine. A solution of 20 mmol of *n*-hexylamine dissolved in 10 ml of dichloroethane was treated with 10 mmol of N_2phF. The reaction mixture was stirred overnight and then washed twice with 1 N HCl and twice with water. The organic phase was dried (by $MgSO_4$), and then ether and chloroform were added until the solution

TABLE I: Elementary Analysis of Dnp Derivatives of Normal and Branched Alkylamines.

	C		H		N	
Hapten	Calcd	Found	Calcd	Found	Calcd	Found
N-Dnp-methylamine	42.64	42.86	3.58	3.75	21.32	21.17
N-Dnp-ethylamine	45.50	45.32	4.30	4.49	19.9	19.72
N-Dnp-propylamine	48.00	48.3	4.92	4.82	18.66	18.56
N-Dnp-Isopropylamine	48.00	48.24	4.92	5.06	18.66	18.81
N-Dnp-butylamine	50.2	50.2	5.48	5.60	17.57	17.65
N-Dnp-*sec*-butylamine	50.2	50.5	5.48	5.59	17.57	17.67
N-Dnp-isobutylamine	50.2	50.39	5.48	5.59	17.57	17.15
N-Dnp-*tert*-butylamine	50.2	50.48	5.48	5.25	17.57	17.17
N-Dnp-dimethylamine	45.5	45.46	4.30	4.41	19.9	19.95
N-Dnp-diethylamine	50.2	49.98	5.48	5.46	17.57	17.50

TABLE II: Elementary Analysis of Dnp Derivatives of the Amino Acids and the Dipeptides Studied.

	C		H		N	
Hapten	Calcd	Found	Calcd	Found	Calcd	Found
N-Dnp-glycine	39.8	39.84	2.90	2.88	17.41	18.00
N-Dnp-(glycine)$_2$	40.27	39.18	3.38	3.68	18.79	18.98
N-Dnp-alanine (L)	42.36	42.30	3.56	3.72	16.47	16.50
N-Dnp-alanine (D)	42.36	42.37	3.56	3.66	16.47	16.50
N-Dnp-(alanine)$_2$ (LL)	44.17	43.51	4.33	4.30	17.17	17.66
N-Dnp-(alanine)$_2$ (DD)	44.17	43.67	4.33	4.48	17.17	17.25
N-Dnp-(alanine)$_2$ (LD)	44.17	43.95	4.33	4.50	17.17	17.40
N-Dnp-(alanine)$_2$ (DL)	44.17	43.95	4.33	4.52	17.17	17.05

became turbid. Crystallization took place at 4° overnight. The crystalline yellow derivative was collected, dried *in vacuo*, and checked for purity by tlc (single spot on plates developed in chloroform) and elementary analysis. *Anal.* Calcd: C, 53.92; H, 6.41; N, 15.72. Found: C, 53.70; H, 6.21; N, 15.4.

1-N-2,4-Dinitrophenylcyclohexylamine. The synthesis of this ligand was carried out as described for the other *N*-Dnp-alkylamines. Only dimethylformamide was used for dissolving the residue after the evaporation step and crystallization, instead of ethanol. *Anal.* Calcd: C, 54.33; H, 5.70; N, 15.84. Found: C, 54.06; H, 5.77; N, 15.39.

1-N-2,4-Dinitrophenyl Derivatives of Benzylamine and 2-Aminoethanol. These ligands were synthesized as described for the alkylamines. For the benzylamine derivative Calcd: C, 57.14; H, 4.06; N, 15.38. Found: C, 56.98; H, 4.13; N, 15.43. For the 2-aminoethanol derivative Calcd: C, 42.0; H, 4.38; N, 18.4. Found: C, 40.70; H, 3.85; N, 18.16.

Alanine dipeptides containing L and D residue at predetermined positions were synthesized as described by Schechter and Berger (1966).

1-N-2,4-Dinitrophenyl Derivatives of Glycine, Glycylglycine, L-Alanine, D-Alanine, and of Four Alanylalanine Dipeptides (LL, DD, LD, DL). A solution of 5 mmol of the respective amino acid or dipeptide, dissolved in 5 ml of water containing 10 mmol of $NaHCO_3$, was treated with 5 mmol of N_2phF dissolved in 10 ml of ethanol. The reaction mixture was stirred for 1 hr at 37° and then 1 ml of concentrated HCl was added to it. The solution was left to crystallize overnight at 4°. The solution was then filtered; the crystals were washed with 1 N HCl and dried *in vacuo*. Products were checked for purity by tlc and elementary analysis (Table II).

Mono-1-N-2,4-dinitrophenyl Derivatives of 1,2-Ethylenediamine and 1,3-Propylenediamine. These ligands were synthesized by a similar procedure as that described for the Dnp derivatives of the alkylamines. The only differences were the use of a high excess of the respective diamine with the N_2phF (40:1) to minimize the formation of the bis-Dnp product, and repeated recrystallizations were carried out. The products were found to be pure by tlc (plates were developed in CH_3OH–CH_3COOH–H_2O (4:1:1) or CCl_4–CH_3OH–CH_3COOH (95:4:1) and elementary analysis. For the ethylenediamine derivative Calcd: C, 42.48; H, 4.46; N, 24.77. Found: C, 42.40; H, 4.32; N, 24.77. For the propylenediamine derivative Calcd: C, 45.00; H, 5.10; N, 23.4. Found: C, 45.12; H, 4.98; N, 23.71.

Methods. Absorption measurements were made in the wavelength range 200–550 nm at 25° on a Cary Model 15 recording spectrophotometer, in cells with 10- or 2-mm light path. *Fluorescence measurements* were carried out on a Turner Model 210 recording spectrofluorometer in rectangular cells with 10- or 4-mm light path, according to Velick *et al.* (1960). The excitation wavelength was 280 nm and emission was measured at 350 nm. Titration data were treated by a computer program written by D. Lancet from our department, based on the Scatchard and Sips equations (Karush, 1962). All data were corrected for nonspecific quenching due to nonspecific binding, by titrating normal rabbit IgG with the corresponding ligand.

Kinetic measurements were carried out on solutions containing protein-315 and the various ligands with a temperature-jump spectrofluorometer (R. Rigler, R. Rabl, and T. Jovin, manuscript in preparation; Pecht *et al.*, 1972a). Changes in the fluorescence of protein-315 excited at 280 nm, due to chemical relaxation, were followed. Cut-off filters were used to eliminate all light shorter than 300 nm. A temperature jump of approximately 5° (from 16 to 21°) was brought about by a capacitor discharge (5×10^{-8} F, 20 kV) through the examined solutions. The specific rate constants were calculated by a computer program assuming a single-step mechanism using the τ values calculated from the slopes of the relaxation curves. No initial guess of K, $k_{12}{}^*$, or $k_{21}{}^*$ was required. The program generated an accurate guess that permitted a rapid minimization scheme (Victor *et al.*, 1973).

Absorbance, fluorescence, and kinetic measurements were done on solutions containing the protein and the ligand at the indicated concentrations in 0.1 M NaCl–0.05 M sodium phosphate buffer (pH 7.4). For ligands with limited solubility in this medium, *e.g.*, Dnp-*N*-alkylamines, a concentrated solution in 50–100% ethanol was prepared and then diluted in the reaction mixture. The ethanol concentration in the reaction mixture was always below 5%.

Model Building Measurements. "Orbit" molecular building set models (R J M Exports Ltd., England) of the different ligands were built and distances between the different substituents on the 2,4-dinitrophenyl ring and the ring were measured. All the given distances were measured from the center of the Dnp ring. Table III summarizes the bond lengths used.

In constructing and measuring the models, attention was paid to the following points. (a) Distance measurements were carried out on the assumed most stable conformation of the compounds, taking into consideration steric factors and interactions between the different groups constituting the ligand. (b) Preference was given to the conformation enabling a hydrogen bond between the hydrogen of the 1-amino group and the oxygen of the 2-nitro group. Wherever such a conformation was regarded as unstable, a conformation in which the N–H or N–R bond of the 1-NH-2,4-dinitrophenyl group is perpendicular to the plane of the ring was preferred for the purpose of distance measurements. (c) Because of the likelihood of free rotation around certain bonds in the ligand

TABLE III: Bond Lengths used for the Molecular Models.

Bond Type	Bond Length (Å)
C–C paraffinic	1.54
C–C in aromatic compounds	1.40
C–N paraffinic	1.47
C–N in the peptide bond	1.32
C–H paraffinic (average value for mono-, di-, and trisubstituted carbon)	1.08
C–H in aromatic compounds	1.08
C=O in carboxylic acids or of the peptide bond	1.36
N–O in NO_2	1.18
N–H of the amino group	1.04

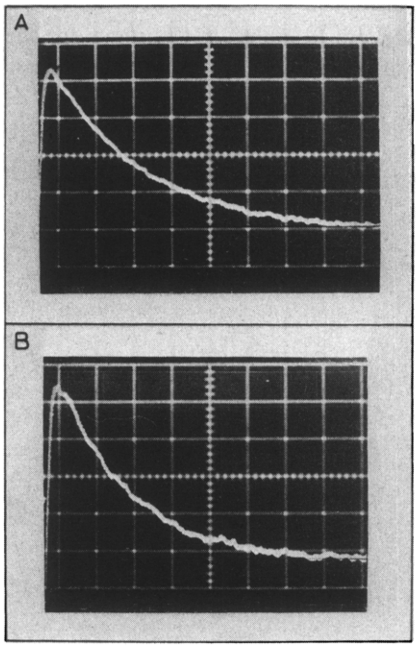

FIGURE 1: Two oscilloscope traces of the fluorescence changes of a system consisting of 1.34×10^{-6} M protein-315 and 1.36×10^{-6} M Dnp-*N*-propylamine (a) and 2.2×10^{-6} M Dnp-*N*-butylamine (b). Sweep rate (a,b), 1 msec/cm, sensitivity (a,b), 50 mV/cm.

molecules, it was not possible to suggest angles or spatial orientations. Thus, the only meaningful parameter can be the distance of a certain group from the center of the Dnp ring. Due to this limitation, the "subsite of interaction" in the protein binding site was located at the measured distance, on the surface of a cylinder of rotation.

Results

The perturbation induced by the temperature jump effected only a single chemical relaxation for all the protein and ligand systems. Two typical oscilloscope traces of the relaxation curves observed during temperature-jump experiments are shown in Figure 1. Experiments carried out in the absence of the ligands showed no relaxation phenomena.

The measured relaxation times over an extensive range of concentrations of both protein and ligand have demonstrated that the reciprocal relaxation time, τ^{-1}, depends linearly on the sum of the free concentrations of the protein and hapten. This dependence of τ^{-1} is in agreement with a single binding mechanism, and is expressed by eq 2 (Eigen and

$$\tau^{-1} = k_{12}^*(\overline{\mathrm{Ab}} + \overline{\mathrm{H}}) + k_{21}^* \tag{2}$$

Maeyer, 1963), where $\overline{\mathrm{Ab}}$ and $\overline{\mathrm{H}}$ are the free concentrations of protein and ligand, respectively. A plot of data obtained for the binding of 1-*N*-2,4-dinitrophenylpropylamine to the myeloma protein is shown in Figure 2. The slope and the intercept of the computed line gave the two rate constants k_{12}^* and k_{21}^*, respectively.

Static equilibrium constants (K_{st}) determined by fluorescence quenching titrations were found to be in good agreement with the "dynamic" equilibrium constants calculated from the ratio of the two rate constants.

Rate and equilibrium constants were derived for the reaction between protein-315 and three different classes of ligands: (a) nitrophenyl ligands differing in the number and position of the nitro groups or in the nature of the substituents on the aromatic ring; (b) 1-amino derivatives of 2,4-dinitrophenyl in which (i) one or both of the amino group hydrogens were substituted by methyl or ethyl groups, (ii) one of these hydrogens was substituted by alkyl chains differing in length and branching, and (iii) one of these hydrogens was substituted by normal alkyl chains carrying a terminal carboxylate or ammonium group; (c) Dnp derivatives of some amino acids and their dipeptides.

(*a*) *Binding of Ligands Differing in Substitutions in the Aromatic Nucleus.* Table IV summarizes the rate and equilibrium constants computed from the relaxation data for the first class of these ligands. Pronounced differences in the affinity between the 2,4-dinitro derivatives and the 2,6-dinitro or *p*-nitro derivatives of aniline or toluene were observed. C-1 substitution of 2,4-Dnp by either N, C, or O did not lead to marked differences in kinetic behavior and the affinity except for the dinitrophenolate ion which is negatively charged. In view of difficulties in a systematic correlation of the kinetic data with the variation in the substitution in the aromatic nucleus, where both topological and electronic density changes are involved, the 1-*N*-2,4-dinitrophenyl was selected as the basic unit of the studied ligands. The absorption spectrum of this nucleus overlaps the protein emission spectrum, and the binding of the ligand can be correlated with the quenching of protein fluorescence (Eisen and Siskind, 1964). Spectral overlap, to the same extent, was also found for the 1-oxy derivatives of 2,4-dinitrobenzene that were studied. These two classes of ligands have strong absorption bands in the

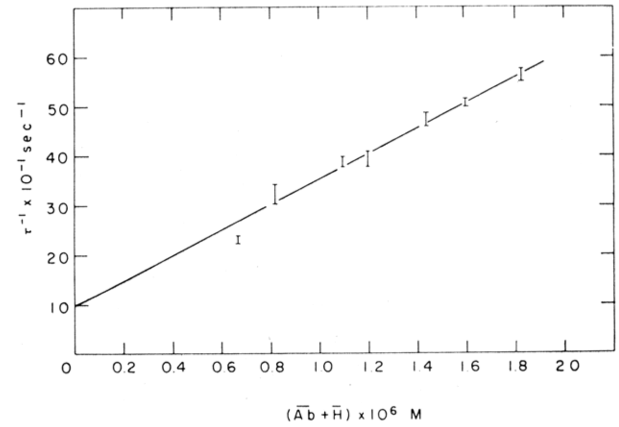

FIGURE 2: The dependence of the observed reciprocal relaxation times on the concentrations of free protein-315 and free Dnp-*N*-propylamine at equilibrium.

TABLE IV: Rate and Equilibrium Constants for the Interaction between Protein-315 of Mono-, Di-, and Trinitrobenzene Substituted at Position 1 by Different Chemical Groups.

	Hapten	$k_{12}^* \times 10^{-8}$ (M^{-1} sec^{-1})	k_{21}^* (sec^{-1})	$K = (k_{12}^*/k_{21}^*) \times 10^{-5}$ (M^{-1})	$K_{st} \times 10^{-5}$ (M^{-1})
1	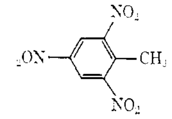	2.2 ± 0.15	284 ± 15	7.8	8.30
2	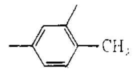	1.4 ± 0.12	1050 ± 90	1.3	1.25
3	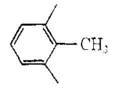				<0.1
4	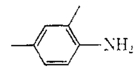	4.8 ± 0.3	927 ± 75	5.1	3.00
5	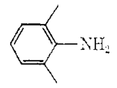				<0.1
6	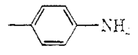				<0.1
7	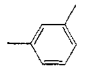				<0.1
8	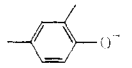				<0.1
9	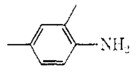	4.8 ± 0.30	927 ± 75	5.1	3.00
10	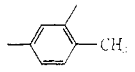	1.4 ± 0.12	1050 ± 90	1.3	1.25
11	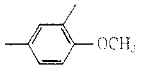				1.70
12	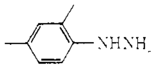	0.84 ± 0.7	723 ± 100	1.16	

300–400-nm region which overlap the 340-nm emission band of the antibodies. In contrast, the spectral overlap of the nitrotoluene derivatives and antibody fluorescence is significantly smaller (Figure 3).

As indicated in Table IV it was impossible to measure by the fluorescence quenching the binding of 2,4-dinitrobenzene and 2,6-dinitrotoluene. This is not due to a lack of overlap between the absorption spectra of these compounds and the emission spectra of the protein (Figure 3) since 2,4-dinitrotoluene and 2,4,6-trinitrotoluene, which have the same extent of spectral overlap (Figure 3), showed measurable amplitudes in the temperature-jump experiments. Hence the negative results obtained with the 2,4-dinitrobenzene and 2,6-dinitrotoluene must be due to low affinity. Of interest in this respect is that no hypochromism and no red shift of the type observed for all the nitroaniline-substituted haptens was found in this study for the nitrotoluene derivatives (Eisen and Siskind, 1964; Little and Eisen, 1966, 1967; Rockey, 1967; Eisen *et al.*, 1968; Painter *et al.*, 1972).

(*b*) *Binding of Dnp Ligands Differing in Their Side Chains.* The reaction between 2,4-dinitroaniline derivatives, in which one or both of the NH_2 group hydrogens were substituted by methyl or ethyl groups, and protein-315 was studied in order to determine the effect of the amino group hydrogens (which are hydrogen bonded to the 2-NO_2 group of Dnp), on the binding and to probe their possible hydrogen bonding to specific amino acid residues in the site (Table V).

The data indicate that the amino group hydrogens are not essential for binding and that specific hydrophobic interactions at this region contribute significantly to the binding of

TABLE V: Rate and Equilibrium Constants for the Interaction between Protein-315 and a Series of Mono- and Disubstituted 1-*N*-Alkyl Derivatives of 2,4-Dinitroaniline.

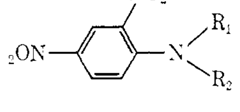

	Hapten		$k_{12}^* \times 10^{-8}$	k_{21}^*	$K = k_{12}^*/k_{21}^*) \times 10^{-5}$
	R_1 =	R_2 =	(M^{-1} sec^{-1})	(sec^{-1})	(M^{-1})
1	H	H	4.8 ± 0.30	927 ± 75	5.10
2	H	CH_3	3.5 ± 0.24	373 ± 30	9.35
3	CH_3	CH_3	3.3 ± 0.20	121 ± 18	27.0
4	CH_2CH_3	CH_2CH_3	2.1 ± 0.15	555 ± 60	3.80

the ligand to the site. However, these interactions are effective only when limited to a certain region. Table VI summarizes the kinetic data for Dnp derivatives of a homologous series of normal and branched alkylamines. Note that both rate constants (k_{12}^* and k_{21}^*) depend, although to different extents, on the nature of the hydrophobic chain attached to the Dnp ring. From the dependence of k_{21}^* on the structure of the side chain of the hapten it can be deduced that hydrophobic interactions occurring at a defined region or location within the protein binding site have an important role in stabilizing the binding site. It appears that with normal aliphatic side chains, a maximum hydrophobic interaction occurs with the butyl (four C) side chain, and that bulky hydrophobic groups adjacent to the Dnp ring contribute to binding.

The effects of electrostatic interactions located in predetermined positions in the ligand molecule on the rate constants for the binding of these haptens to the protein are summarized in Table VII. The results demonstrate that replacing a neutral hydrophobic group with a charged group can drastically affect the equilibrium binding constant mainly by changing the dissociation rate constant of the specific ligand. The neutral 1-*N*-2,4-dinitrophenylethylamine (1) is 15 times more strongly bound to the protein-315 binding site than the negatively charged homolog 1-*N*-2,4-dinitrophenylglycine (2). On the other hand, the neutral 1-*N*-2,4-dinitrophenylbutylamine (8) is about 2.6 times less strongly bound than its negatively charged homolog, the 1-*N*-2,4-dinitrophenyl derivative of γ-aminobutyric acid (9). The charge dependence of the dissociation rate expressed in Table VII is a good illustration of the transition from a hydrophobic subsite to an electrostatic subsite. Thus, at a distance of 6–7 Å from the center of the Dnp ring hydrophobic interactions are favored whereas at a distance of 8 Å electrostatic interactions are favored.

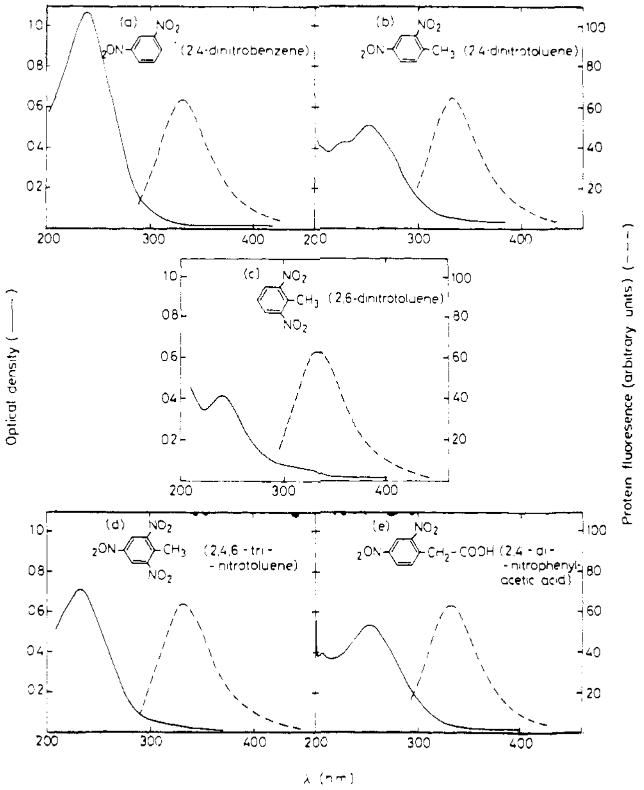

FIGURE 3: Spectral overlap of the emission spectrum of protein-315 with the absorption spectra of various nitrotoluene derivatives.

(*c*) *Binding of Dnp Peptides Differing in Their Stereospecificity.* To analyze the effect of the spatial arrangement of certain hydrophobic and charged groups in the combining site the kinetics of binding of a series of diastereoisomeric peptides were studied. In Figure 4, the linearity of the dependence of τ^{-1} on the sum of the free concentrations of hapten and protein is illustrated for this type of ligands. From these plots and from the data in Table VIII, it is evident, as found for all the other groups of ligands reported in this study, that both k_{12}^* and k_{21}^* depend on the chemical nature and the three-dimensional structure of the ligand.

A careful analysis of Tables VII and VIII enabled us to locate a "subsite of electrostatic interactions," and to probe with higher accuracy the influence and position of the other types of interactions within the binding site.

Discussion

(*a*) *Is the Antibody–Hapten Reaction Diffusion Controlled?* That the rate-determining step in the hapten–antibody reaction is diffusion controlled has been proposed by Day *et al.*

TABLE VI: Rate and Equilibrium Constants for the Interaction between Protein-315 and (1) a Homologous Series of Dnp-alkylamines and (2) Dnp Derivatives Containing Branched, Cyclic, or Aromatic Side Chains.

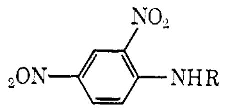

	R =	$k_{12}^* \times 10^{-8}$ (M^{-1} sec^{-1})	k_{21}^* (sec^{-1})	$K = (k_{12}^*/k_{21}^*) \times 10^{-6}$ (M^{-1})	$K_{st} \times 10^{-6}$ (M^{-1})
1	CH_3	3.5 ± 0.24	373 ± 30	0.94	
2	CH_2CH_3	2.8 ± 0.18	143 ± 24	1.95	2.04
3	$CH_2CH_2CH_3$	2.6 ± 0.18	94 ± 11	2.70	
4	$CH_2CH_2CH_2CH_3$	2.5 ± 0.3	79 ± 10	3.20	3.40
5	$CH_2CH_2CH_2CH_2CH_2CH_3$	1.2 ± 0.12	123 ± 18	1.00	1.10
6	$CH(CH_3)_2$	3.7 ± 0.22	108 ± 8.6	3.40	
7	$CH(CH_2CH_2)_2CH_2$	2.55 ± 0.25	116 ± 10	2.20	
8	$CH_2CH(CH_3)_2$	2.0 ± 0.14	83 ± 11	2.40	2.70
9	$C(CH_3)(CH_3)_2$	3.6 ± 0.3	58 ± 6	6.10	
10	CH_2Ph	1.8 ± 0.15	47 ± 9	3.80	

TABLE VII: Rate and Equilibrium Constants for the Interaction between Protein-315 and a Homologous Series of Dnp Derivatives Containing Electrostatically Charged Side Chains.

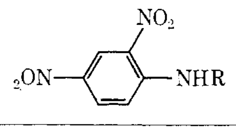

	Hapten, R =	$k_{12}^* \times 10^{-8}$ (M^{-1} sec^{-1})	k_{21}^* (sec^{-1})	$K = (k_{12}^*/k_{21}^*) \times 10^{-5}$ (M^{-1})	$K_{st} \times 10^{-5}$ (M^{-1})
1	CH_2CH_3	2.8 ± 0.18	143 ± 24	19.5	20.4
2	CH_2COO^-	1.7 ± 0.18	1340 ± 100	1.27	2.0
3	$CH(CH_3)COO^-$	2.4 ± 0.2	664 ± 80	3.60	2.67
4	$CH_2CH_2CH_3$	2.6 ± 0.18	94 ± 11	27.0	
5	CH_2CH_2OH	2.5 ± 0.3	370 ± 50	6.75	6.6
6	$CH_2CH_2COO^-$	1.8 ± 0.3	285 ± 50	6.40	
7	$CH_2CH_2NH_3^+$	0.65 ± 0.1	735 ± 65	0.89	1.3
8	$(CH_2)_3CH_3$	2.5 ± 0.3	79 ± 10	32.0	34.0
9	$(CH_2)_3COO^-$	3.8 ± 0.2	45 ± 9	84.0	
10	$(CH_2)_3NH_3^+$	0.83 ± 0.08	850 ± 100	0.98	
11	$(CH_2)_4COO^-$	1.2 ± 0.3	55 ± 5	22.0	19.0
12	$(CH_2)_5CH_3$	1.2 ± 0.12	123 ± 18	10.0	11.0
13	$(CH_2)_5COO^-$	1.2 ± 0.12	60 ± 10	20.0	
14	$(CH_2)_6NH_3^+$	0.9 ± 0.02	120 ± 10	7.5	

(1963), on the basis of their measured rate constants. According to Froese and Sehon (1965) the difference found between the measured specific binding rate constants (10^8 M^{-1}/sec^{-1}) and the theoretically calculated limiting value (1–2 × 10^9 M^{-1}/sec^{-1}) was small enough to indicate that the antibody–hapten reaction is a diffusion controlled one. This one order of magnitude difference was interpreted by Sehon (1963) and by Pecht *et al.* (1972a) as an indication for some steric restrictions and electrostatic repulsions.

It should be emphasized, however, that the theoretical calculation of the limiting bimolecular rate constant for a diffusion-controlled process involves a large number of assumptions concerning the shape, charge, solid angle of approach, and other parameters of the reacting species (Smoluchowski, 1917; Debye, 1942; Verwey and Overbeek, 1948; Alberty and Hammes, 1958). Depending on the approximations used, theoretical values differing by two orders of magnitude (10^8–10^{10} M^{-1} sec^{-1}) can result.

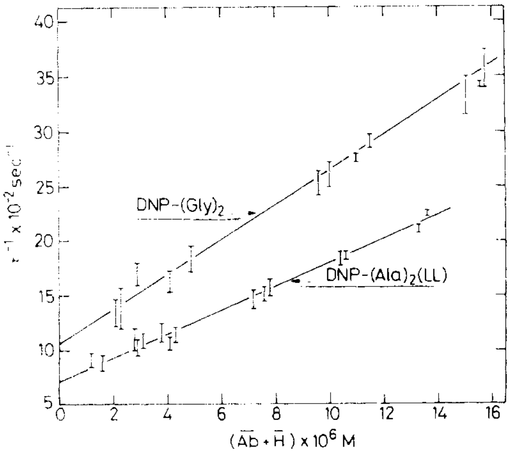

FIGURE 4: The dependence of the observed reciprocal relaxation times on the concentrations of free protein-315 and free Dnp-glycylglycine and free Dnp-L-alanyl-L-alanine at equilibrium.

The data presented in this study correlating the physical and chemical properties of the different ligands, and the k_{12}^* values measured for their binding, enabled a careful analysis of the question of whether the antibody–hapten reaction is diffusion controlled.

Our results clearly show that for ligands of very similar structure k_{12}^* varies within one order of magnitude (6.5 × 10^7–4.8 × 10^8 M^{-1} sec^{-1}). Substituting the dimethylamino group (Table V, 3) by the diethylamino group (Table V, 4) leads to a 40% decrease in k_{12}^*. Both ligands are neutral and very similar in all their physical and chemical properties, so that any difference in their diffusion coefficients or their radius can be neglected. Changing the aliphatic hydrocarbon chain attached to the Dnp ring from a methyl to an *n*-hexyl side chain also brings about a pronounced decrease (66%) in k_{12}^* (Table VI). The only difference between the first five ligands of Table VI is the length of the aliphatic chain attached to the Dnp ring. The difference in the diffusion coefficient of the *N*-methylamine and *N*-hexylamine derivatives cannot explain the difference in k_{12}^* between the two ligands since it would be more than compensated by the increase in size. Even more conclusive is the comparison between ligands 6, 8, and 9 in Table VI. The k_{12}^* for the isobutylamine derivative (8) is 54% lower than the k_{12}^* value measured for the isopropylamine (6) and *tert*-butylamine (9) derivatives. No significant differences in either diffusion coefficient or reaction cross-section are expected between these ligands.

Note the k_{12}^* values measured for the charge ligands presented in Table VII. Comparing ligands 1 and 2 and 4 and 5, it is evident that the binding rate constants for the negatively charged ligands are 30–40% lower than those of the uncharged homologs. The k_{12}^* values observed for the positively charged ligands (ligands 7 and 10) were the lowest rate constants measured. There is a 3–5-fold difference between their binding rate constant and the k_{12}^* measured for the neutral homologs, ligands 4 and 8. The observation that the k_{12}^* values for positively charged ligands are lower than those

TABLE VIII: Rate and Equilibrium Constants for the Interaction between Protein-315 and Dnp Derivatives of Amino Acids and Dipeptides.

1-*N*-2,4-Dinitrophenyl Derivatives of	$k_{12}^* \times 10^{-8}$ ($\text{M}^{-1}\ \text{sec}^{-1}$)	k_{21}^* (sec^{-1})	$K = (k_{12}^*/k_{21}^*) \times 10^{-5}$ (M^{-1})	$K_{\text{st}} \times 10^{-5}$ (M^{-1})
Gly-COO$^-$	1.7 ± 0.18	1340 ± 100	1.27	
(Gly$\!\!\rightarrow\!_2$COO$^-$	1.6 ± 0.15	1058 ± 100	1.50	
Ala-COO$^-$ (L)	2.4 ± 0.2	664 ± 80	3.60	2.67
(Ala$\!\!\rightarrow\!_2$COO$^-$ (LL)	1.1 ± 0.12	721 ± 50	1.52	
(Ala$_2\!\!\rightarrow$COO$^-$ (LD)	1.47 ± 0.2	880 ± 120	1.67	1.80
Ala-COO$^-$ (D)	1.15 ± 0.1	314 ± 25	3.66	
(Ala$\!\!\rightarrow\!_2$COO$^-$ (DD)	2.25 ± 0.4	470 ± 43	4.80	4.20
(Ala$\!\!\rightarrow\!_2$COO$^-$ (DL)	1.4 ± 0.24	335 ± 40	4.2	

measured for the uncharged homologs indicates that the binding process is not diffusion controlled and is highly influenced by the protein net charge, since protein-315 is negatively charged at this pH. This is further illustrated by the differences in k_{12}^* within the series of the homologous aliphatic derivatives discussed above. There are several examples of ligands with identical or similar k_{21}^* which differ by 3–4 times in their k_{12}^* (*e.g.*, ligands 3 and 7 or 9 and 11 in Table VII).

This analysis of the binding rate constants (k_{12}^*) clearly indicates that any interpretation of the pronounced differences in k_{12}^* must consider factors other than differences in the diffusion coefficients of the reactants or in their reaction radius. It demonstrates that the antibody–hapten reaction is more complex than just a simple bimolecular, diffusion-controlled combination.

(*b*) *Two-Step Mechanism for the Antibody–Hapten Reaction.* A more realistic picture of the antibody–hapten (ligand) reaction may be achieved by introducing an additional step.

$$\underset{\text{(encounter)}}{\text{Ab} + \text{H} \underset{k_{21}}{\overset{k_{12}}{\rightleftharpoons}} \text{Ab}\cdots\text{H}} \underset{\text{(transformation)}}{\underset{k_{32}}{\overset{k_{23}}{\rightleftharpoons}} \text{AbH}} \qquad (3)$$

In this treatment k_{12}^*, the binding rate constant, is expressed by two consecutive steps. First is the fast, diffusion-controlled encounter step influenced mainly by the rate of diffusion of the reactants, their charges, and reaction distance. The second is the transformation step. In this presentation the magnitude of k_{23} is determined by the various interactions within the Ab···H complex en route to the site while that of k_{32} reflects the degree of complementarity between the binding site and the ligand. This rate is influenced by the following factors: (a) spatial symmetry of the reacting molecules, (b) steric factors, (c) binding site rigidity, and (d) specific repulsive or attractive interactions.

In the proposed two-step binding mechanism there is a diffusion-controlled bimolecular formation of a loosely bound "encounter complex" followed by a unimolecular step in which the final antibody–hapten complex is formed (transformation) (eq 3). In this system one should observe two relaxation times. However, under conditions where the concentration of the intermediate complex Ab···H is small compared with the concentrations of Ab, H, or AbH, the equilibrium between Ab + H and AbH is characterized by one relaxation time only (Eigen *et al.*, 1964)

$$\tau = (k_{21} + k_{23})/k_{12}(\overline{\text{Ab}} + \overline{\text{H}})k_{23} + k_{32}k_{21} \qquad (4)$$

$$\tau^{-1} = k_{12}^*(\overline{\text{Ab}} + \overline{\text{H}}) + k_{21}^*$$

where $k_{12}^* = k_{12}k_{23}/(k_{21} + k_{23})$ and $k_{21}^* = k_{32}k_{21}/(k_{21} + k_{23})$. This seems to be the case for the antibody–hapten reaction.

The model presented above is supported by the kinetic data obtained by Pecht *et al.* (1972a). Using the temperature-jump method they measured the binding of dinitrophenyllysine to the homogeneous protein-315. The Fab fragments and the intact molecules, which differ somewhat in their diffusion coefficients but have exactly the same binding site, had the same binding rate constant. Since the above measurements were carried with the same hapten and the same binding site, and since in the proposed kinetic model the rate-determining step of the association reaction is the transformation step, which must be identical for the Fab and for the intact molecule, there is full agreement between the experimental data and the proposed model. There is, however, some disagreement between this model and the data presented by Kelly *et al.* (1971). Using the temperature-jump and the stopped-flow techniques they measured rate and equilibrium constants for the reaction of conventionally induced rabbit anti-dinitrophenyl antibodies or their Fab fragments with two Dnp derivatives. For both haptens the value of k_{12}^* for the Fab was twice that observed with the whole intact molecules. This change is greater than would have been expected on the basis of the difference in the diffusion coefficients of the intact molecules and its Fab fragment.

(*c*) *Mapping the Subsites of Interaction.* (i) *Dnp Ring Subsite.* From the data presented in Table IV it is clear that for the formation of a stable complex between a nitrophenyl ligand and the site of protein-315, at least positions 2 and 4 of the phenyl ring must be substituted by nitro groups. When only the para (4) position or when both positions 2 and 6 are substituted, the affinity of the ligands is very low (below $10^4\ \text{M}^{-1}$). This is true for both the 1-NH_2 and 1-CH_3 substituted nitrophenyl derivatives. It seems that the nitro group in positions 2 and 4 cause the interactions needed for the formation of the stable complex. This is similar to the results reported by Eisen and Siskind (1964) for induced anti-2,4-dinitrophenyl antibodies, and in agreement with the general trend found by Nisonoff *et al.* (1959) for anti-3,5-dinitrophenyl antibodies.

Another interesting observation resulted from the comparison of spectral properties of the 2,4-dinitro derivatives of aniline and toluene. Although they both exhibit similar affinity and fluorescence quenching, the nitrotoluene ligands did not show the well-known hypochromic effect and red shift of their absorptions. This is in contrast to the results of Eisen and Siskind (1964) who found hypochromism and red shift for a nitrotoluene derivative reacting with induced anti-Dnp antibodies.

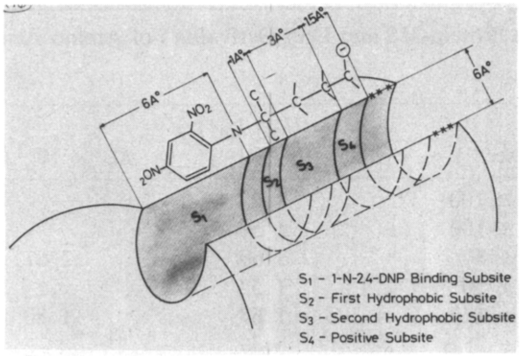

FIGURE 5: A model of the binding site of protein-315 showing the four subsites of interaction.

From the kinetic parameters for four derivatives of 2,4-dinitroaniline in which one or both amino hydrogens were replaced by methyl or ethyl groups (Table V) we can conclude the following. First, these data eliminate the possible requirement for a hydrogen bond formation between the ligands, amino group and an appropriate group in the site. Second, they show that the major effect of the substitutions by methyl groups is a pronounced decrease in k_{21}*. It seems reasonable according to these data that hydrophobic interactions between ligands of this size and the site play an important stabilizing role in the formation of the ligand–site complex. That these interactions are limited by certain topological factors is evident from the high value of the k_{21}* measured for the diethylamine derivative. As the diethyl derivative was the widest ligand studied in this work the high k_{21}* value found for it (555 sec^{-1}) was attributed to its difficulty to fit the site. This observation led us to estimate the width of the site as ~6 Å.

In this discussion we have neglected the direct effects of the different substituents on the properties of the aromatic ring itself and so on its binding to the site. From the models of the methyl and diethyl derivatives it is clear that substituting the amino hydrogens by the two more bulky alkyl groups results in twisting the substituent group relative to the plane of the benzene ring. As was shown by Godfrey and Murrell (1964), twisting of this type will have two effects. First, the resonance integral will be reduced and second, the inductive effect of the substituent may change. The dimethylamino group is π-electron repelling but σ-electron attracting. Rotating this group will cause reduction of the π-electron inductive effect. At a large angle of twist this may also change its sign. For the exact calculations of their influence on specific electrostatic and charge-transfer interactions involved in the binding, it is necessary to know the accurate wave functions for the interacting molecules or residues and to assume a model for the binding site. Attempts to calculate such values are at the beginning and are far from being unequivocal (New and Richards, 1972; Rein and Pack, 1973).

Detailed analysis of the kinetic data contained in Tables VI and VII, and especially of the dissociation rate constants (k_{21}*), enabled us to characterize the binding site of protein-315 in terms of the subsite of interaction concept. The binding site can be divided into several subsites of interactions. Each subsite is defined as a region located in a certain distance from the Dnp binding region, in which interactions of a specific type (electrostatic, hydrophobic, charge transfer, etc.) take place between the ligand and certain amino acid residues (Figure 5). This approach is based on the assumption that the different ligands are positioned in the binding site in such a way that the Dnp ring always occupies the same region. This region (the Dnp binding subsite) is our reference point for the coming analysis, and is designated in the proposed model by S_1. In the light of affinity labeling experiments (Givol *et al.*, 1971, 1972; Haimovich *et al.*, 1972) this assumption seems valid, and implies a rigid structure in the active site of protein-315, fixed positioning of the Dnp moiety, and a large degree of immobilization of the bound haptens. The hypochromism and red shift in absorbance exhibited by all the 1-*N*-2,4-dinitrophenyl derivatives upon binding suggests interaction of the 1-*N*-2,4-dinitrophenyl group bound at its binding subsite S_1 with the indole ring of a tryptophanyl residue (Little and Eisen, 1967).

TABLE IX: Position Analysis Correlating the Assumed Conformations of the Dnp Derivatives of Glycine, L-Alanine, and D-Alanine with Their Dissociation Rate Constants.[a]

	P_1	P_2	P_3	P_4	
	Distance (Å)				k_{21}*
	3–4	4–5	5–6	6–7	(sec^{-1})
Dnp-NH-Gly	CH_2		C	O_2^-	1340
Dnp-NH-Ala (L)	CH	CH_3	C	O_2^-	664
	CH	CH_3			
Dnp-NH-Ala (D)	C				314
		O_2^-			

[a] The position of each group on the ligand (p) is the distance (Å) of this group from the center of the Dnp ring as measured in model compounds.

In order to further evaluate the interactions of the different ligands with the binding site we considered the side chains attached to the 1-NH-Dnp group in terms of the distance, measured in Å, between the different carbon, nitrogen, or oxygen atoms composing the side chain and geometric center of the Dnp group. This distance is defined as the position (p) of these groups and is designated by p_1, p_2, p_3, etc., as the distance from the ring center increases (Table IX–XI).

(ii) *Hydrophobic Subsite.* The presence of a defined hydrophobic subsite in the myeloma protein-315, suggested by the data tabulated in Table V, is further supported by the data presented in Table VI for the binding of the different normal and branched alkylamine derivatives. In Figure 6a,b the dependence of the rate constants and of the overall equilibrium constants on the length of the aliphatic hydrophobic chains (measured from the center of the aromatic nucleus) is shown. In part c of Figure 6, the dependence of k_{21}* on the position (and dimensions) of a compact hydrophobic nucleus in the ligand molecule is illustrated.

The optimum length of the aliphatic side chains attached to the 1-*N*-2,4-dinitrophenyl group is reflected in the minimum value of k_{21}* observed for a chain length which extends to a distance of 6–8 Å from the center of the Dnp binding subsite (Figure 6a). The minimum in k_{21}* and the decrease in k_{12}* resulting from the elongation of the aliphatic side chain produced a well-defined maximum in the overall equilibrium constant. The presence of a branched hydrophobic nucleus in the hapten molecule positioned 4–5 Å from the ring center (Figure 6c) lowered the minimum value of k_{21}*, indicating the stabilizing effects of hydrophobic interactions in this location.

TABLE X: Position Analysis Correlating the Assumed Conformations of the Dnp Derivatives of Glycylglycine, L-Alanyl-D-alanine, and D-Alanyl-L-alanine with Their Dissociation Rate Constants.

	p_1	p_2	p_3	p_4	p_5	p_6	p_7	
				Distance (Å)				
	3–4	4–5	5–6	6–7	7–8	8–9	9–10	k_{21}^* (sec^{-1})
Dnp-NH-(Gly)$_2$	CH$_2$		C(=O)	NH	CH$_2$	C	O$_2^-$	1058
Dnp-NH-(Ala)$_2$ (LD)	CH	CH$_3$	C(=O) NH	CH CH$_3$	C	O$_2^-$		880
Dnp-NH-(Ala)$_2$ (DL)	CH	CH$_3$	C(=O) NH		CH CH$_3$ C	O$_2^-$		335

TABLE XI: Position Analysis Correlating Assumed Conformations of the Dnp Derivatives of L-Alanyl-L-alanine and D-Alanyl-D-alanine with Their Dissociation Rate Constants.

	p_1	p_2	p_3	p_4	p_5	p_6	
				Distance (Å)			
	3–4	4–5	5–6	6–7	7–8	8–9	k_{21}^* (sec^{-1})
Dnp-NH-(Ala)$_2$ (LL)	CH CH$_3$		C(=O) NH		CH CH$_3$	C O$_2^-$	721
Dnp-NH-(Ala)$_2$ (DD)	CH	CH$_3$	C(=O) NH	CH	C CH$_3$	O$_2^-$	470

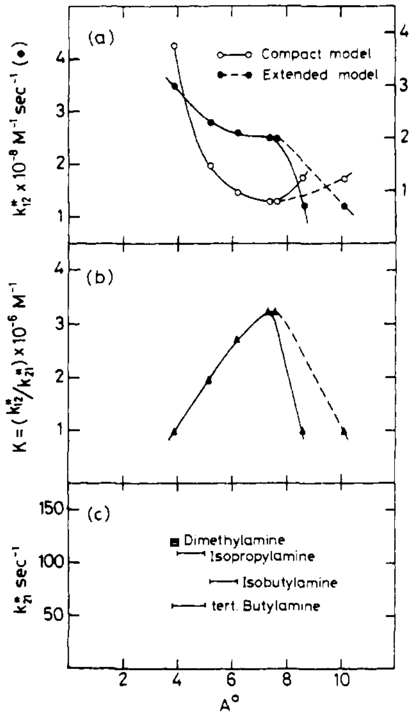

FIGURE 6: The dependence of k_{12}^*, k_{21}^*, and K on the length of normal aliphatic side chains measured from the center of the Dnp ring (a) and (b). (c) The dependence of k_{21}^* on the distance and dimensions of a hydrophobic nucleus from the center of the Dnp ring (see Table VI). Two types of models were analyzed, the compact model and the extended one.

When such a branched nucleus is located 6–8 Å from the center of the ring the values of k_{21}^* increases, indicating that the hydrophobic interactions at this location are weaker than at 4–5 Å from the center of the ring. Therefore, the hydrophobic subsite in the proposed model was visualized as composed of two regions, the first hydrophobic subsite (S$_2$) (4–5 Å from the center of the ring) which exhibits stronger binding interactions, and the second hydrophobic subsite (S$_3$) (6–8 Å from the center of the ring) which has weaker interactions with the hydrophobic moieties of the ligand.

(iii) *Positive Subsite.* It was pointed out by Schechter (1972) that, in principle, information of a more precise nature on the properties of binding sites can be derived from comparing haptens of equal size which differ from one another in one particular feature like charge or stereospecificity, rather than from studying the effect of elongation in a homologous series, as was done for the aliphatic alkylamine derivatives. This is because effects caused by the elongation are not necessarily due to the contribution of the added group, but can also be attributed to changes in favorable or unfavorable interactions functioning in the smaller haptens.

Accordingly, rate and equilibrium constants were determined for haptens of the same size, but which differ from one another in their charge (Table VII). The changes in k_{12}^* and k_{21}^* as well as the changes in the overall equilibrium constant as a function of the distance of a terminal carboxyl group from the center of the Dnp ring is illustrated in Figure 7. The curves are based on the kinetic data for different Dnp derivatives of aliphatic acids (ligands 2, 6, 9, 11, 12) differing in the length of their aliphatic chain.

It is not possible to explain the complex dependence of k_{12}^* on the distance of the COO$^-$ group from the binding subsite, because of the intrinsic difficulties in distinguishing charges located in the site from charges distributed throughout the whole protein molecule, and in finding the exact conformation of these ligands in solution and in the binding site. The dependence of k_{21}^* on the distance of the COO$^-$ group, together with the other kinetic data (Table VII), enabled us to characterize a subsite where electrostatic interactions play an important role. The rather high values of k_{21}^* observed when the negative carboxylate group is close to the to the aromatic nucleus (5–7 Å) can be explained by assuming the existence of electrostatic repulsions between the negatively charged ligands and negatively charged residues in the site, or by assuming a lack of appropriately charged residues in this location. The data proposing the existence of a hydrophobic subsite exactly in this region support the second explanation. The steep decrease of k_{21}* upon increasing the distance of the carboxylate ion from the aromatic nucleus and the minimum exhibited when this group is located 8.5–9.5 Å from the center of the Dnp ring may result from the presence of positively charged residues in the site in this region. The high k_{21}* values measured for the positively charged homologs (ligands 7 and 10, Table VII) are a further support for this notion. Repulsive interactions between these positive haptens and some positively charged residues in the site will cause this unstable binding expressed by the high k_{21}* values. These data permit us to define the "positive subsite" (S_4) located 8.5–9.5 Å from the center of the Dnp binding subsite (S_1).

More precise mapping of the different interacting groups in the site can be achieved by comparing the binding of ligands differing in their three-dimensional structure. Data concerning such a comparative study are collected in Table VIII. Many questions can be raised regarding these results, of them the following three are the most interesting. (1) Why is k_{21}* for (Dnp-Gly) > k_{21}* for (Dnp-L-Ala) > k_{21}* for (Dnp-D-Ala)? (2) Why is k_{21}* for (Dnp-(Gly)$_2$) > k_{21}* for (Dnp-(Ala)$_2$)DD > k_{21}* for (Dnp-(Ala)$_2$)DL? (3) Why is k_{21}* for (Dnp-(Ala)$_2$)LL > k_{21}* for (Dnp-(Ala)$_2$)DD?

In order to answer these questions, analysis of the structures of these ligands in terms of the position concept (introduced in this discussion) was made by comparing model compounds. Table IX contains the data needed for answering the first question. In this table, the only meaningful structural difference between Dnp-glycine and Dnp-L-alanine is the existence in the Dnp-L-alanine of a methyl group positioned 4–5 Å from the center of the Dnp ring. This position corresponds exactly to the place where, according to the preceding analysis, strong hydrophobic interactions between hapten and protein are favorable. These interactions lead to an approximately 50% decrease in the k_{21} of the L-alanyl derivative compared with the glycyl derivative. It is noteworthy that k_{21}* of the D-Ala derivative is half that of the L-Ala derivative. This may indicate an assymmetry of the site in this region which is more complementary to the methyl group of the D diastereoisomer. One should also consider the possibility that the carboxylate groups of the two isomers are placed in different positions and these, *via* electrostatic interactions, also stabilize the complex.

Table X contains the data necessary for the analysis of the second question. The lower k_{21}* (higher stability) measured for the dialanine derivative in which the sequence is LD compared with the diglycine derivative can be attributed to the spatial arrangement of the different groups composing the alanylalanine derivative. The structure of this ligand leads to the positioning of (a) the negative charge in the positive subsite (8–9 Å), and (b) the methyl group in the first hydrophobic subsite (4–5 Å). This complementarity of the reacting groups is also the main reason for the even lower k_{21}* value observed for the Dnp-DL-alanylalanine. Positioning of an additional hydrophobic group at the second hydrophobic subsite, 7–8 Å away from the center of the Dnp binding subsite, as well as the same positioning of the negatively charged carboxyl oxygens and of the methyl group, as found for the LD form, leads to an almost threefold decrease in the dissociation rate constant. These data further support the proposed subsite of interaction model.

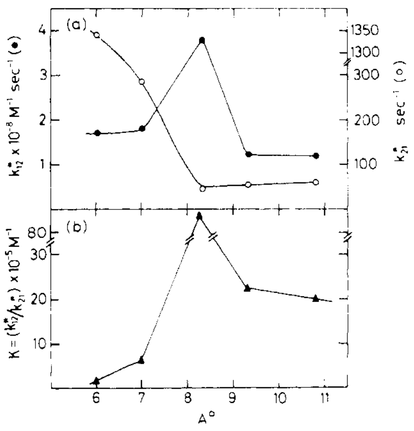

FIGURE 7: The dependence of k_{12}*, k_{21}*, and K on the distance of the carboxyl group of the aliphatic side chain from the center of the Dnp ring (a) and (b) (see Table VII). Only the extended model of the molecules was analyzed.

It is more difficult to answer the third question and to explain the 1.5-fold decrease in k_{21} found for the DD-dialanine diastereoisomer compared with the LL diastereoisomer (Table XI). It seems that the presence of the hydrophobic groups (CH_3 and CH) 4–5 and 6–7 Å away from the Dnp binding subsite, respectively, in the regions defined previously, contribute to a stronger stability of the complex between protein-315 and the DD dipeptide. A comparison of the rate constants of Dnp-diglycine and Dnp-δ-aminovaleric acid (both of the same size) shows that the k_{21}* of the diglycine derivative is about 20 times higher. This must be due to the presence of a peptide bond at a distance of 5–7 Å from the center of the Dnp ring in the diglycine derivative (Table X). At this distance hydrophobic interactions were found to be favorable and therefore the peptide bond at this location will cause a decrease in affinity. A similar behavior (high k_{21}* values) was observed also for the other dipeptides.

Concluding Remarks

The general picture of the combining site of protein-315 emerging from our kinetic mapping studies, though more detailed, is similar to that obtained by Siskind and Eisen (1964) on induced Dnp antibodies. This and other studies permit us to draw some conclusions about the antibody combining site and the antibody–hapten reaction.

(1) The binding site seems to be quite rigid and its complementarity with various ligands is inherent in its structure. No mechanism such as "induced fit" or "extensive motility" is required in order to stabilize the complex with its ligand.

(2) Although the Dnp ring contributes the major part of the free energy of binding, there is also a significant contribution by the side chain attached to it. This allows us to locate certain areas of interactions in the site, clearly separated one from another, which are defined as subsites of interactions (Figure 5).

(3) The combining site of protein-315 can be divided on the basis of the kinetic data into four subsites of interactions, whose location in the protein sequence can be evaluated with the help of affinity labeling experiments. (i) Affinity labeling with nitrene derivatives of Dnp ligand (Fleet *et al.*, 1972) and paired labeling of antibodies to different, aromatic haptens (Takeda *et al.*, 1974; Friedensen *et al.*, 1972; Roholt

et al., 1973) indicate that the major area of complementary to the benzene ring is the third hypervariable region in both the L and H chain. The noncovalent bonds between the Dnp ring and the amino acid residues within the site seem to be due to hydrophobic and charge-transfer interactions as well as hydrogen bonds in a nonaqueous environment (Eisen and Siskind, 1964). In view of other affinity labeling studies (Haimovich *et al.*, 1972) it is possible that the charge-transfer interactions involves tryptophan-49 and tryptophan-37 in the H chain and L chain, respectively. (ii) The presence of a positively charged subsite at a distance of 8–9.5 Å from the center of the Dnp ring binding subsite is in good agreement with the affinity labeling (Haimovich *et al.* 1972) of Lys-54 in the H chain by the bromoacetyl derivative of Dnp-lysine (BADL). Although BADL is 3 Å longer it may be folded in the site into a more compact form. The identification of a positive subsite at about this distance is evidence that Lys-54 and the second hypervariable region are involved in complementarity with the "tail" of the Dnp ligands. (iii) Between the two complementary areas mentioned above, there is a region which provides mainly hydrophobic interactions. Any charged group or even a peptide bond will not be favored in this area and its free energy of binding will decrease markedly.

(4) The association between antibody and hapten is not a simple diffusion-controlled process and therefore the association constant (K) does not contain all the information necessary for the comparative analysis of the interaction between different ligands and the antibody. The different association rate constant (k_{12}^*) indicate the presence of a short-lived encounter complex which is followed by the entrance of the ligand into the site with the formation of a stable complex. The dissociation rate constant (k_{21}^*) is the reciprocal of the complex lifetime and therefore provides information on interactions within the combining site.

(5) The fact that only one relaxation effect was observed for all the hapten–MOPC 315 systems studied here can be interpreted as evidence against the existence of any major conformational change in the antibody molecule upon hapten binding.

References

Abramovitz, N., Schechter, I., and Berger, A. (1967), *Biochem. Biophys. Res. Commun. 29*, 862.

Alberty, R. A., and Hammes, G. G. (1958), *J. Phys. Chem. 62*, 154.

Atlas, D., Levit, S., Schechter, I., and Berger, A. (1970), *FEBS* (*Fed. Eur. Biochem. Soc.*) *Lett. 11*, 281.

Barisas, B. G., Singer, S. J., and Sturterant, J. M. (1974), (in press).

Berger, A., and Schechter, I. (1970), *Phil. Trans. Roy. Soc. London, Ser. B 257*, 249.

Cuatrecasas, P., Wilchek, M., and Anfinsen, C. B. (1968), *Science 162*, 1491.

Day, L. A., Sturtevant, J. M., and Singer, S. J. (1962), *J. Amer. Chem. Soc. 84*, 3768.

Day, L. A., Sturtevant, J. M., and Singer, S. J. (1963), *Ann. N. Y. Acad. Sci. 103*, 619.

Debye, P. (1942), *Trans. Electrochem. Soc. 82*, 265.

Eigen, M., Kruse, W., Maass, G., and Maeyer, L. de (1964), *Progr. React. Kinet. 2*, 287.

Eigen, M., and Maeyer, L. de (1963), *Tech. Org. Chem. 8*, 793.

Eisen, H. N., Michaelides, M. C., Underdown, B. J., Schulenberg, E. P., and Simms, E. S. (1970), *Fed. Proc., Fed. Amer. Soc. Exp. Biol. 29*, 78.

Eisen, H. N., Simms, E. S., and Potter, M. (1968), *Biochemistry 7*, 4126.

Eisen, H. N., and Siskind, G. (1964), *Biochemistry 3*, 996.

Fleet, G. W. J., Knowles, J. R., and Porter, R. R. (1972), *Biochem. J. 128*, 499.

Friedensen, B., Appella, E., Roholf, D. A., and Pressman, D. (1972), *Biochem. Biophys. Res. Commun. 48*, 1208.

Froese, A. (1968), *Immunochemistry 5*, 253.

Froese, A., and Sehon, A. H. (1965), *Immunochemistry 2*, 135.

Froese, A., Sehon, A. H., and Eigen, M. (1962), *Can. J. Chem. 40*, 1786.

Givol, D., Strausbauch, P. H., Hurwitz, E., Wilchek, M., Haimovich, J., and Eisen, H. N. (1971), *Biochemistry 10*, 3461.

Givol, D., Wilchek, M., Eisen, H. N., and Haimovich, J. (1972), Immunoglobulins, Amsterdam, North-Holland Publishing Co., p 77.

Godfrey, M., and Murrell, J. N. (1964), *Proc. Roy. Soc., Ser. A, 278*, 71.

Haimovich, J., Eisen, H. N., Hurwitz, E., and Givol, D. (1972), *Biochemistry 11*, 2389.

Haimovich, J., Givol, D., and Eisen, H. N. (1970), *Proc. Nat. Acad. Sci. U. S. 67*, 1656.

Haselkorn, D., Pecht, I., Friedman, S., Yaron, A., Givol, D., and Sela, M. (1971), *Isr. J. Chem. 9*, 53.

Hochman, J., Inbar, D., Wilchek, M., Pecht, I., and Givol, D. (1972), *Isr. J. Med. Sci. 8*.

Inbar, D., Hochman, J., and Givol, D. (1972), *Proc. Nat. Acad. Sci. U. S. 69*, 2659.

Inbar, D., Rotman, M., and Givol, D. (1971), *J. Biol. Chem. 246*, 6272.

Kabat, E. A. (1960), *J. Immunol. 84*, 82.

Karush, F. (1962), *Advan. Immunol. 2*, 1.

Kelly, K. A., Sehon, A. H., and Froese, A. (1971), *Immunochemistry 8*, 613.

Kunkel, H. G. (1965), *Harvey Lect. 59*, 219.

Levison, S. A., Portmann, A. J., Kierszenbaum, F., and Dandliker, W. B. (1971), *Biochem. Biophys. Res. Commun. 43*, 258.

Little, J. R., and Eisen, H. N. (1966), *Biochemistry 5*, 3385.

Little, J. R., and Eisen, H. N. (1967), *Biochemistry 6*, 3119.

New, R. R., and Richards, W. G. (1972), *Nature* (*London*), *New Biol. 237*, 214.

Nisonoff, A., Shaw, A. R., and Pressman, D. (1959), *J. Amer. Chem. Soc. 81*, 1418.

Painter, R. G., Harvey, J. S., and Tanford, C. (1972), *Biochemistry 11*, 1327.

Pecht, I., Givol, D., and Sela, M. (1972a), *J. Mol. Biol. 68*, 241.

Pecht, I., and Haselkorn, D. (1971), *Isr. J. Chem. 9*, 52.

Pecht, I., Haselkorn, D., and Friedman, S. (1972b), *FEBS* (*Fed. Eur. Biochem. Soc.*) *Lett. 24*, 331.

Potter, M., Dreyer, W. J., Kuff, E. L., and McIntire, K. R. (1964), *J. Mol. Biol. 8*, 814.

Pressman, D., and Grossberg, A. (1968), The Structural Basis of Antibody Specificity, New York, N. Y., W. A. Benjamin.

Rein, R., and Pack, G. R. (1973), *Nature* (*London*) *242*, 526.

Roholt, O. A., Takeda, Y., Friedensen, B., Appella, E., and Pressmann, D. (1973), *Fed. Proc., Fed. Amer. Soc. Exp. Biol. 32*, 4149.

Rockey, J. H. (1967), *J. Exp. Med. 125, 249*.

Schechter, I. (1970), *Eur. J. Biochem. 14*, 516.

Schechter, I. (1972), *Ann. N. Y. Acad. Sci. 190*, 129.

Schechter, I., and Berger, A. (1966), *Biochemistry 5*, 3362.

Schechter, I., and Berger, A. (1967), *Biochem. Biophys. Res. Commun. 27*, 157.

Schechter, I., and Berger, A. (1968), *Biochem. Biophys. Res. Commun. 32*, 898.

Schneider, H., and Sehon, A. H. (1961), *Trans. N. Y. Acad. Sci. 24*, 15.

Sehon, A. H. (1963), *Ann. N. Y. Acad. Sci. 103*, 626.

Sharon, N., and Chipman, D. M. (1969), *Science 165*, 454.

Smoluchowski, M. V. (1917), *Z. Phys. Chem. 92*, 129.

Sturtevant, J. M., Wofsy, L., and Singer, S. J. (1961), *Science 134*, 1434.

Takeda, J., Friedensen, B., Roholt, O. A., and Pressman, D. (1974) (in press).

Underdown, B. J., Simms, E. S., and Eisen, H. N. (1971), *Biochemistry 10*, 4359.

Velick, S. F., Parker, C. W., and Eisen, H. N. (1960), *Proc. Nat. Acad. Sci. U. S. 46*, 1470.

Verwey, E. J., and Overbeek, J. T. G. (1948), Theory of the Stability of Lyophilic Colloids, Amsterdam, Elsevier.

Victor, J., Haselkorn, D., and Pecht, I. (1973), *Comput. Biomed. Res. 6*, 121.

Conformational Transitions in Glycogen Phosphorylase Reported by Covalently Bound Pyridoxamine Derivatives†

Knut Feldmann, Bernhard J. M. Gaugler, Heinz Winkler,‡ and Ernst J. M. Helmreich*

ABSTRACT: $NaBH_4$ reduced rabbit skeletal muscle phosphorylases *b* and *a* (α-1,4-glucan:orthophosphate glycosyltransferase (EC 2.4.1.1.)) dissociate on acidification completely to monomers. The conformational change leading to the disruption of the interprotomeric bonds is reported by the absorbance and fluorescence of the bound pyridoxamine-5′-P and analogs modified at the 5′ position. The structural alteration was shown to involve changes in dimer conformations followed by monomerization. A comparison of the responses to pH of several reduced phosphorylase derivatives carrying the pyridoxamine—the 5′-deoxypyridoxamine methylenephosphonate—and the pyridoxamine 5′-monomethyl ester analogs indicated that the ionization of the 5′ group is not related to the structural change. Neutralization (or 5′-AMP addition) completely reversed the pH perturbation of reduced phosphorylases resulting in reassociation of monomers to oligomers and in reactivation, the rate of which was enhanced by substrates. 5′-AMP and substrates also protected against inactivation by acidification. But, in the absence of 5′-AMP substrates alone were ineffective. The absorbance and fluorescence intensity of reduced phosphorylase *b* at a given pH (6.25) was concentration dependent whereas the quantum yield was independent of concentration. This together with the change of the fluorescence intensity of glutardialdehyde cross-linked reduced dimer *b* with pH change indicated that the spectral properties including the fluorescence polarization of bound pyridoxamine-5′-P are the same in the monomer and in at least one of the dimeric forms. This makes it unlikely that the chromophore is buried between the two subunits and can only be exposed on dissociation. The spectral properties of the cofactor in oligomeric reduced phosphorylases *b* and *a* at neutral pH can be explained without assuming that the chromophore is completely immersed in a hydrophobic crevasse. The structure of the binding site must only enable the 3′-OH group of the cofactor to be hydrogen bonded. There is no convincing reason why other protonatable groups, especially the 5′-P moiety, could not react in a more hydrophilic environment.

Pyridoxal-5′-P is essential for the activity of all known α-glucan phosphorylases, but its function is not known (Fischer *et al.*, 1970). But whatever its role one has to bear in mind that the pyridoxamine-5′-P derivative which is covalently linked to phosphorylase as secondary amine is still active (Fischer *et al.*, 1958). This should make $NaBH_4$-reduced phosphorylase a suitable object for the study of pyridoxal-5′-P function.

Cortijo and Shaltiel (1970) reported that the quantum yield of the fluorescence of bound pyridoxamine-5′-P in reduced phosphorylase *b* increased about 10-fold when the pH was lowered from 7.0 to 5.8. The pH effect was interpreted as to result from a conformational change of the enzyme. This stimulated us to study the nature of the conformational change which reduced phosphorylase undergoes on lowering pH and which is reversed by 5′-AMP (see Johnson *et al.*, 1970).

On the basis of previous experiments on the role of 5′-AMP in phosphorylase activation (Helmreich and Cori, 1964a,b; Helmreich *et al.*, 1967; Kastenschmidt *et al.*, 1968a,b), it seemed likely that in the case of reduced phosphorylase the allosteric nucleotide would also affect conformational transitions between active and inactive forms. Recently we could show that the phosphorylase monomer bound to Sepharose is nearly inactive (Feldmann *et al.*, 1972). This led us to a study of monomer–oligomer equilibria in reduced phosphorylase which verified the suggestion of Jones and Cowgill (1971) that reduced phosphorylase *b* and as is shown here *a* as well, dissociate on acidification to monomers and reassociate slowly on addition of 5′-AMP (or neutralization). Substrates (mainly glycogen) enhanced reassociation and reactivation but

---

† The Department of Physiological Chemistry, The University of Würzburg School of Medicine, 87 Würzburg, Germany. *Received October 16, 1973.* This work was supported by grants from the DFG (He 22), the VW Foundation, the Federal Ministry of Science and Technology and the Fonds der Chemie. Preceding papers on the role of pyridoxal 5′-phosphate in glycogen phosphorylase are: Pfeuffer *et al.* (1972a,b), Weisshaar and Palm (1972), and Feldmann *et al.* (1972). A preliminary report of some aspects of this study has appeared (Ehrlich *et al.*, 1973).

‡ The Max-Planck-Institute of Biophysical Chemistry, Karl-Friedrich-Bonhoeffer-Institute, Göttingen-Nikolausberg, Germany.